

## High-spin states in $^{166}\text{Lu}$

D. Hojman,<sup>(1)\*</sup> A. J. Kreiner,<sup>(1,2)</sup> M. Davidson,<sup>(2)</sup> J. Davidson,<sup>(2)</sup> M. Debray,<sup>(1,2)</sup> E. W. Cybulska,<sup>(3)</sup>  
P. Pascholati,<sup>(3)</sup> and W. A. Seale<sup>(3)</sup>

<sup>(1)</sup>*Departamento de Física, Comisión Nacional de Energía Atómica, 1429 Buenos Aires, Buenos Aires, Argentina*

<sup>(2)</sup>*Departamento de Física, Facultad de Ciencias Exactas y Naturales, Universidad de Buenos Aires, Buenos Aires, Argentina*

<sup>(3)</sup>*Instituto de Física, Universidade de São Paulo, São Paulo, Brazil*

(Received 21 May 1991)

High-spin states belonging to  $^{166}\text{Lu}$  have been studied through the  $^{159}\text{Tb}(^{12}\text{C},5n)$  fusion-evaporation reaction in the energy range  $E(^{12}\text{C})=75\text{--}90$  MeV. In-beam and activity singles spectra and  $\gamma\text{--}\gamma\text{--}t$  coincidences have been measured. A completely new level scheme is proposed. Each rotational band is interpreted on the basis of coupling scheme systematics.  $g\text{--}S$  crossing frequencies and alignments have been extracted.  $B(M1)/B(E2)$  reduced transition probability ratios have been calculated using a semi-classical method and compared to the experimental values.

PACS number(s): 21.10.Re, 23.20.Lv, 27.70.+q

### I. INTRODUCTION

High-spin spectroscopy of doubly odd nuclei, belonging to the deformed heavy rare-earth region, has become, in the last decade, of interest for the investigation of rotational phenomena. Until now, the work performed was focused on Tl (Refs. [1,2]), Ir (Refs. [3–5]), Re (Refs. [6–8]), and Ta (Refs. [9,10]) isotopes. This work has contributed to the development of a classification [11] of rotational structures in doubly odd nuclei, many of which are very distorted if compared to a normal behavior [i.e., the  $I(I+1)$  law]. Another point of interest in the study of a doubly odd nucleus has been the observation of changes in the crossing frequency between the  $S$  and  $g$  bands [12] for different quasiparticle configurations [13].

The present work is a contribution in the neutron-deficient region of still higher deformation and level density where very little information is available. Part of the results presented here has already been reported [14]. The only hitherto known information [15] for  $^{166}\text{Lu}$  was the existence of three isomeric states with spins and parities  $6^-$ ,  $3^-$ , and  $0^-$  ( $T_{1/2}=2.65, 1.41, \text{ and } 2.12$  min) and several low-spin states populated through the decay of  $^{166}\text{Hf}$ .

### II. EXPERIMENTS

The search for high-spin states belonging to  $^{166}\text{Lu}$  was performed through the  $^{159}\text{Tb}(^{12}\text{C},5n)$  fusion-evaporation reaction at the TANDAR Tandem Laboratory of the Atomic Energy Commission in Buenos Aires.

The set of experiments is comprised of the following: (a) An excitation function in the energy range  $E(^{12}\text{C})=75\text{--}90$  MeV using a self-supporting 4 mg/cm<sup>2</sup> Tb foil. (b) In-beam and activity singles spectra at  $E(^{12}\text{C})=82$  MeV, using two Ge detectors of 30 and 40 %

efficiency surrounded by BGO Compton suppressors and a high-resolution planar detector. Figure 1 shows an in-beam singles spectrum measured with the last-mentioned counter placed at 90° to the beam direction. Due to its extreme complexity, only the most important  $\gamma$  rays have been indicated. The study of the decay spectra showed that the most populated isomeric state is the  $6^-$ . This is consistent with what we can expect in a fusion-evaporation reaction using heavy ions. (c) Two  $\gamma\text{--}\gamma$  coincidence experiments were performed. For the first, a conventional  $\gamma\text{--}\gamma\text{--}t$  coincidence experiment using the two Compton suppressed Ge detectors,  $25 \times 10^6$  events were recorded in magnetic tapes and  $\gamma\text{--}\gamma$  matrices were constructed with and without timing conditions. Due to the presence of a large number of multiplets and the bad time resolution at low  $\gamma$ -ray energies of the large volume counters, another  $\gamma_1\text{--}\gamma_2\text{--}\gamma_3\text{--}t_{12}\text{--}t_{13}\text{--}t_{23}$  coincidence was performed. In this case the Compton suppressed 30% Ge, the planar, and an x detector were used. There were approximately  $40 \times 10^6$  registered events. (d) An angular distribution measurement with a 1.2 mg/cm<sup>2</sup> self-supporting Tb target was carried out. The beam energy was  $E(^{12}\text{C})=80.5$  MeV and the counters used were the 30% Ge and the planar, placed at (90°, 110°, 125°, 135°, 150°) and (25°, 40°, 55°, 75°, 90°), respectively. Unfortunately, the good resolution, the Compton suppression, and the high statistics of the singles spectra could not overcome its complexity and reliable values for the angular distribution coefficients could not be extracted.

Table I gives  $\gamma$ -ray energies,  $\gamma$ -ray and total intensities according to the assigned multipolarities for the  $^{159}\text{Tb}(^{12}\text{C},5n)^{166}\text{Lu}$  reaction at 82 MeV. In the case of weak or unresolved transitions, the intensities were obtained from coincidence spectra. The multipolarities were assigned on the basis of intensity balances and rotational arguments (see the next two sections).

### III. LEVEL SCHEME

The assignment of  $\gamma$ -rays to  $^{166}\text{Lu}$  was based on excitation functions, coincidences with Lu x rays, and previous

\*Present address: Institut de Physique Nucléaire, Université Paris-Sud, 91406 Orsay CEDEX, France.

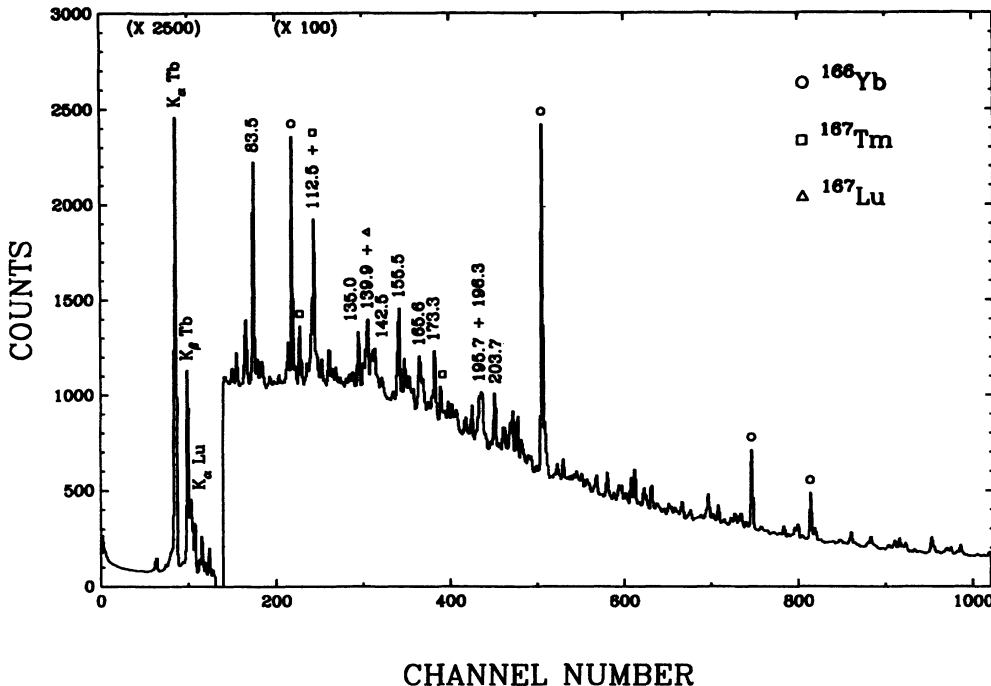


FIG. 1. In-beam singles spectrum for the  $^{159}\text{Tb}(^{12}\text{C},xn)$  reaction at 82 MeV, measured with a high-resolution planar detector. Only the most important  $\gamma$  rays have been indicated.

knowledge of the neighboring Lu isotopes, i.e.,  $^{165,167}\text{Lu}$  (Refs. [16,17]). With the data obtained we have constructed the completely new level scheme shown in Fig. 2. This high-spin level scheme mainly consists of two  $\Delta I=1$  cascades (*A, B*) and two  $\Delta I=2$  sequences (*C, D*), probably linked by two weak transitions (162.4 and 251.3 keV). Figures 3 and 4 show summed coincidence spectra for the *A* and *B* bands.

The ground state (g.s.) of  $^{166}\text{Lu}$  has  $I^\pi=6^-$  (Ref. [15]) and, as said, is the state which is by far the most populated in the present work. The first line above the g.s. is an 83.5 keV, *E1* isomeric transition. It is in delayed coincidence with the rest of the level scheme, being the only  $\gamma$  ray with a measurable half-life. Its values was determined by two different methods. The centroid shift [18] between the 83.5 and 85.5 keV (prompt transition) lines gives  $T_{1/2}=92(7)$  ns. A similar value was obtained from the slope of the 83.5 keV time spectrum [ $T_{1/2}=91(8)$  ns]. Figures 5(a) and (b) show the 83.5 and 85.5 keV time spectra. In their work on  $^{165}\text{Lu}$ , Jónsson and co-workers [16] determined the half-life of an 83 keV transition as  $T_{1/2}\approx 100$  ns. This transition was not placed in the  $^{165}\text{Lu}$  level scheme and is likely to have been erroneously attributed to  $^{165}\text{Lu}$ . This half-life implies a hindrance factor  $F_w=1.3\times 10^5$  with respect to the Weisskopf estimate for an 83.5 keV *E1* transition. This is consistent with systematics [18] for *E1*,  $|\Delta K|\leq 2$  transitions. It should be stressed, however, that the *E1* character follows unambiguously from intensity balance.

All bands identified in  $^{166}\text{Lu}$  are clearly in coincidence with the 83.5 keV line from the isomeric state (which, for

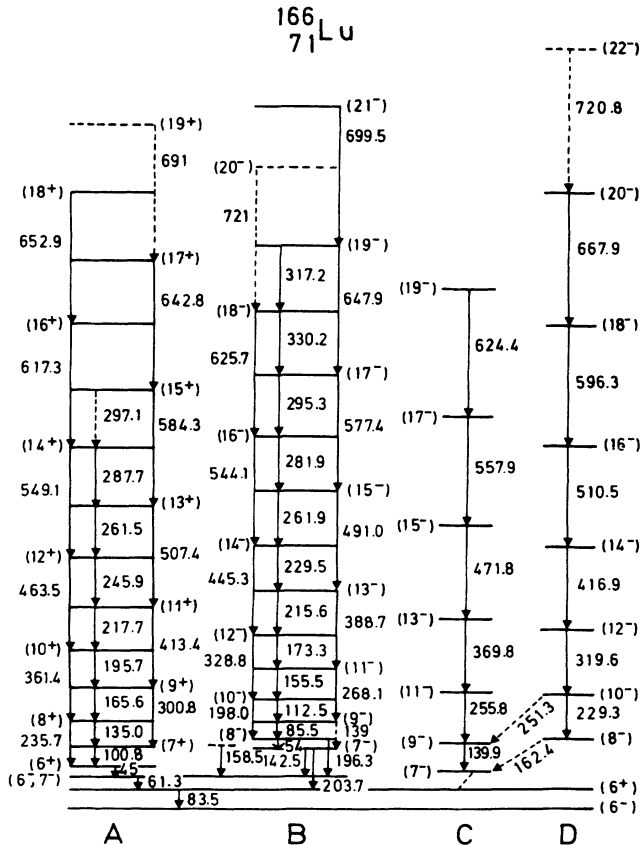


FIG. 2. High-spin level scheme proposed for  $^{166}\text{Lu}$ .

TABLE I.  $\gamma$ -ray energies and intensities, total transition intensities according to the assigned multipolarities for the  $^{159}\text{Tb}(^{12}\text{C},5n)^{166}\text{Lu}$  reaction at 82 MeV.

$E_\gamma^a$ (keV)	$I_\gamma^b$ (arb. units)	$I_t^b$ (arb. units)	Adopted multipolarity
45			<i>E1</i>
54			<i>M1(E2)</i>
61.3	479 <sup>c</sup>	590	<i>E1</i>
83.5	640	1000	<i>E1</i>
85.5	81	567	<i>M1(E2)</i>
100.8	89	427	<i>M1(E2)</i>
112.5	131	489	<i>M1(E2)</i>
115	46		
135.0	86	226	<i>M1(E2)</i>
139			<i>E2</i>
139.9	{ < 87 <sup>d</sup>	< 172	<i>E2</i>
142.5	74	178	<i>M1(E2)</i>
155.5	169	352	<i>M1(E2)</i>
158.5	73	81	( <i>E1</i> )
160.7	50		
162.4	27	53	<i>M1(E2)</i>
165.6	66 <sup>c</sup>	126	<i>M1(E2)</i>
172	37		
173.3	139	251	<i>M1(E2)</i>
181.3	45		
195.7	66	104	<i>M1(E2)</i>
196.3	100	129	<i>M1</i> or <i>E2</i>
198.0	< 39 <sup>d</sup>	< 51	<i>E2</i>
203.7	< 117 <sup>d</sup>	< 124	<i>E1</i>
215.6	105	152	<i>M1(E2)</i>
217.7	55 <sup>c</sup>	78	<i>M1(E2)</i>
229.3	56 <sup>c</sup>	67	<i>E2</i>
229.5	79 <sup>c</sup>	108	<i>M1(E2)</i>
235.7	62	72	<i>E2</i>
245.9	72	94	<i>M1(E2)</i>
251.3			<i>M1(E2)</i>
255.8	82	92	<i>E2</i>
261.5	40 <sup>c</sup>	51	<i>M1(E2)</i>
261.9	75 <sup>c</sup>	95	<i>M1(E2)</i>
268.1	57	63	<i>E2</i>
281.9	79	95	<i>M1(E2)</i>
287.7	35 <sup>c</sup>	42	<i>M1(E2)</i>
295.3	51	60	<i>M1(E2)</i>
297.1			<i>M1(E2)</i>
300.8	72	78	<i>E2</i>
317.2	36 <sup>c</sup>	42	<i>M1(E2)</i>
319.6	69	73	<i>E2</i>
328.8	67	71	<i>E2</i>
330.2	40 <sup>c</sup>	46	<i>M1(E2)</i>
361.4	80	84	<i>E2</i>
369.8	66	69	<i>E2</i>
388.7	88	91	<i>E2</i>
413.4	89	91	<i>E2</i>
416.9	77	79	<i>E2</i>
445.3	98	100	<i>E2</i>
463.5	73 <sup>c</sup>	74	<i>E2</i>
471.8	43 <sup>c</sup>	44	<i>E2</i>
491.0	56 <sup>c</sup>	57	<i>E2</i>
507.4	28 <sup>c</sup>	29	<i>E2</i>
510.5	70 <sup>c</sup>	71	<i>E2</i>
544.1	64 <sup>c</sup>	65	<i>E2</i>
549.1	45 <sup>c</sup>	46	<i>E2</i>

(Table I. *Continued.*)

$E_\gamma^a$ (keV)	$I_\gamma^b$ (arb. units)	$I_t^b$ (arb. units)	Adopted multipolarity
557.9	25 <sup>c</sup>	25	<i>E2</i>
577.4	43 <sup>c</sup>	44	<i>E2</i>
584.3	33 <sup>c</sup>	33	<i>E2</i>
596.3	56 <sup>c</sup>	56	<i>E2</i>
617.3	31 <sup>c</sup>	32	<i>E2</i>
624.4	23 <sup>c</sup>	24	<i>E2</i>
625.7	55 <sup>c</sup>	55	<i>E2</i>
642.8	31 <sup>c</sup>	32	<i>E2</i>
647.9	51 <sup>c</sup>	52	<i>E2</i>
652.9	30 <sup>c</sup>	31	<i>E2</i>
667.9	39 <sup>c</sup>	40	<i>E2</i>
699.5	29 <sup>c</sup>	29	<i>E2</i>
720.8	39 <sup>c</sup>	39	<i>E2</i>

<sup>a</sup> $0.1 \leq \Delta E_\gamma \leq 0.3$  keV.

<sup>b</sup> $10\% \leq \Delta I \leq 30\%$ .

<sup>c</sup>From coincidence spectra.

<sup>d</sup>Multiple peak. Multiplet intensity.

simplicity, has been assumed to be depopulated by the 83.5 keV  $\gamma$  ray). No interband transitions have been found between the *A* and *B* bands, but their relative position could be determined from several transitions linking their bandheads with the ( $6^-, 7^-$ ) and ( $6^+$ ) states which are connected by the 61.3 keV line.

Band *A* deexcites through the 45 and 61.3 keV lines. These transitions are observed, in spectra in coincidence with transitions above them, to stand out clearly amidst of the Lu *K $\beta$*  and Tb *K $\alpha$*  lines. In those spectra, intensi-

ty balances indicate *E1* character for both transitions. Unfortunately, no  $\gamma$ -ray intensity has been obtained for the 45 keV line since it is not well observed in singles spectra or in spectra in coincidence with transitions below it.

Band *B* mainly depopulates through the 142.5 (*M1*), 158.5 (*E1*), 196.3 (*M1* or *E2*), and 203.7 (*E1*) transitions. The indicated multiplicities follow again from intensity balance considerations. The coincidence relations among these lines (and the weak 139 keV crossover) indi-

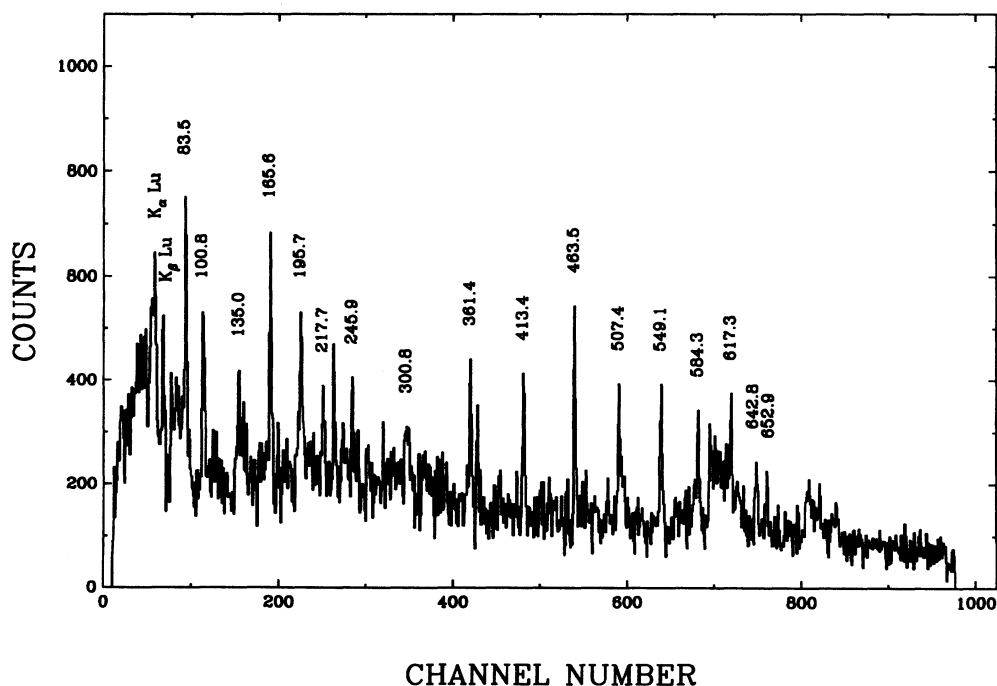


FIG. 3. Added coincidence spectra for the *A* band.

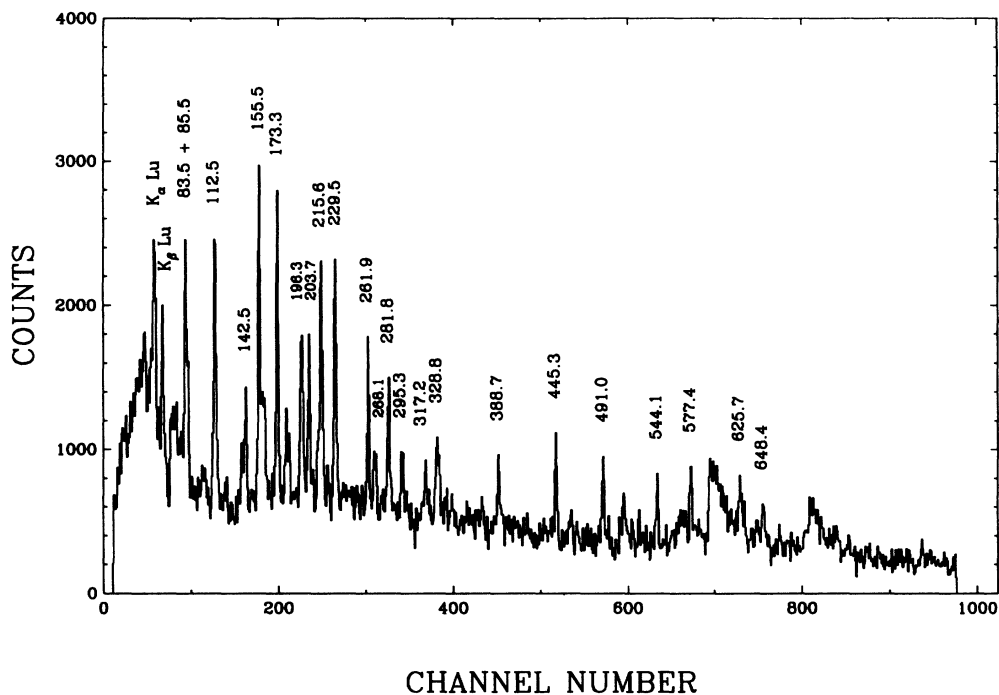


FIG. 4. Added coincidence spectra for the *B* band.

cate the presence of the 54 keV transition which is likely to be the first of band *B*. The nonobservation of this transition is consistent with a highly converted *M1* character. There are other weak transitions depopulating the ( $7^-$ ) and ( $8^-$ ) states of the *B* band (115, 160.7, 172, and 181.3 keV lines), but their exact placement in the level scheme

could not be determined.

As already stated, bands *C* and *D* also depopulate through the 83.5 keV isomeric line. These bands are placed in Fig. 2 at a certain excitation energy above the 83.5 keV level as required by our configuration assignments (see next section). There is an apparent intensity

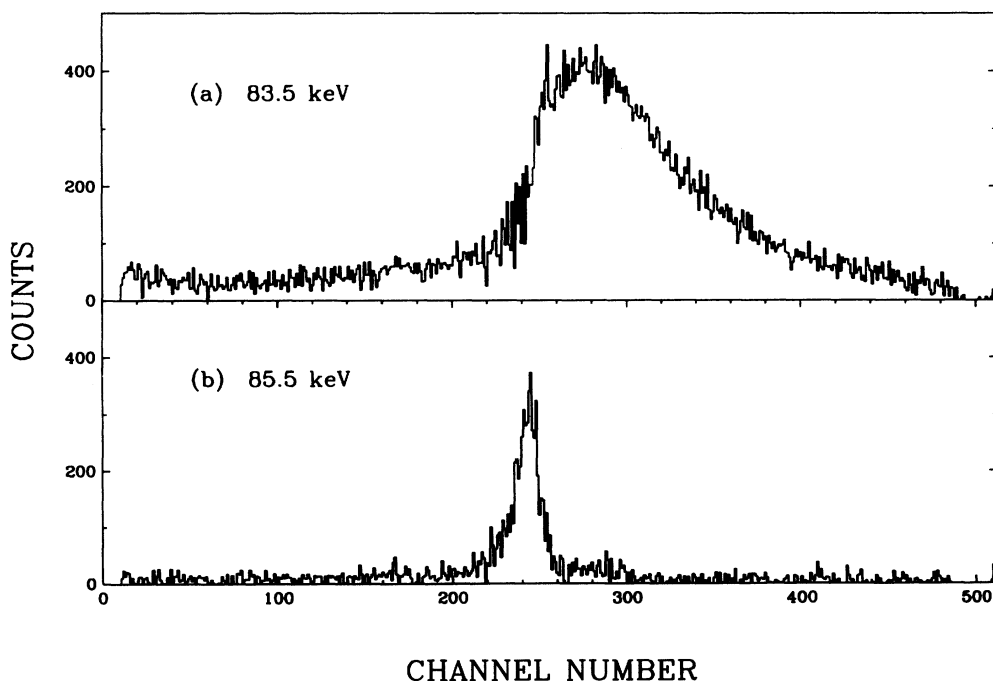


FIG. 5. Time spectra for (a) 83.5 keV transition, (b) 85.5 keV transition.

TABLE II. Zero-order level scheme for  $^{166}\text{Lu}$ .  $K_{\pi}$  values and excitation energies are given.

$E$ (MeV) <sup>d</sup> / $\tilde{\pi}$	$\tilde{\nu}$ $E$ (MeV)	$\frac{5}{2}^{-}$ [523] 0 <sup>a</sup>	$i_{13/2}$ 0.063 <sup>a</sup>	$\frac{3}{2}^{-}$ [521] 0.121 <sup>b</sup>	$\frac{5}{2}^{-}$ [512] 0.213 <sup>c</sup>	$\frac{1}{2}^{-}$ [521] 0.324 <sup>b</sup>
$\frac{7}{2}^{+}$ [404] 0	$K = 6^{-}, 1^{-}$ 0	$6^{+}, 1^{+}$ 0.063	$5^{-}, 2^{-}$ 0.121	$6^{-}, 1^{-}$ 0.213	$4^{-}, 3^{-}$ 0.324	
$\frac{1}{2}^{+}$ [411] 0	$3^{-}, 2^{-}$ 0	$3^{+}, 2^{+}$ 0.063	$2^{-}, 1^{-}$ 0.121	$3^{-}, 2^{-}$ 0.213	$1^{-}, 0^{-}$ 0.324	
$\frac{5}{2}^{+}$ [402] 0.003	$5^{-}, 0^{-}$ 0.003	$5^{+}, 0^{+}$ 0.066	$4^{-}, 1^{-}$ 0.124	$5^{-}, 0^{-}$ 0.216	$3^{-}, 2^{-}$ 0.327	
$\frac{1}{2}^{-}$ [541] 0.226	$3^{+}, 2^{+}$ 0.226	$3^{-}, 2^{-}$ 0.289	$2^{+}, 1^{+}$ 0.347	$3^{+}, 2^{+}$ 0.439	$1^{+}, 0^{+}$ 0.550	
$\frac{9}{2}^{-}$ [514] 0.272	$7^{+}, 2^{+}$ 0.272	$7^{-}, 2^{-}$ 0.335	$6^{+}, 3^{+}$ 0.393	$7^{+}, 2^{+}$ 0.485	$5^{+}, 4^{+}$ 0.596	

<sup>a</sup>Neutron energy corresponds to the average value of  $^{165}\text{Yb}$  and  $^{167}\text{Hf}$ .

<sup>b</sup>Neutron energy corresponds to  $^{165}\text{Yb}$ .

<sup>c</sup>Neutron energy corresponds to  $^{167}\text{Yb}$ .

<sup>d</sup>Proton energies correspond to the average values of  $^{165}, ^{167}\text{Lu}$ .

imbalance in the population and depopulation of the ( $9^{-}$ ) and ( $10^{-}$ ) states belonging to the  $C$  and  $D$  bands, respectively. This is probably due to the presence of unobserved highly converted transitions.

The spins and parities shown in Fig. 2 are not the only possible choice from a strict experimental point of view. They are tentatively assigned from theoretical arguments presented in the next section. Finally, it should be mentioned that none of the transitions hitherto known from the decay of  $^{166}\text{Hf}$  have been observed here.

#### IV. DISCUSSION

The starting point for the discussion of the rotational structures found for an odd-odd nucleus, like  $^{166}\text{Lu}$ , is the construction of a zero-order level scheme (Table II) using single-quasiparticle (qp) energies from neighboring odd nuclei. Their bandhead excitation energies versus neutron number are shown in Fig. 6 for Lu isotopes [16,17,19,20] and in Fig. 7 for Yb isotopes [21–24]. Only states with  $E_{\text{ex}} \leq 600$  keV have been included. The pro-

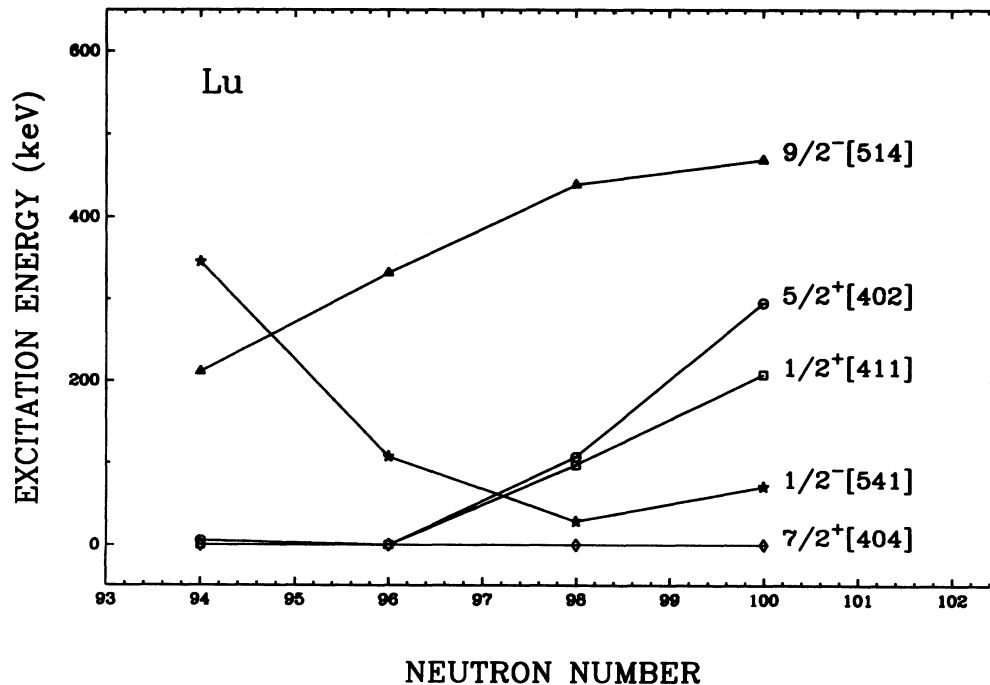


FIG. 6. Bandhead excitation energies for odd Lu isotopes.

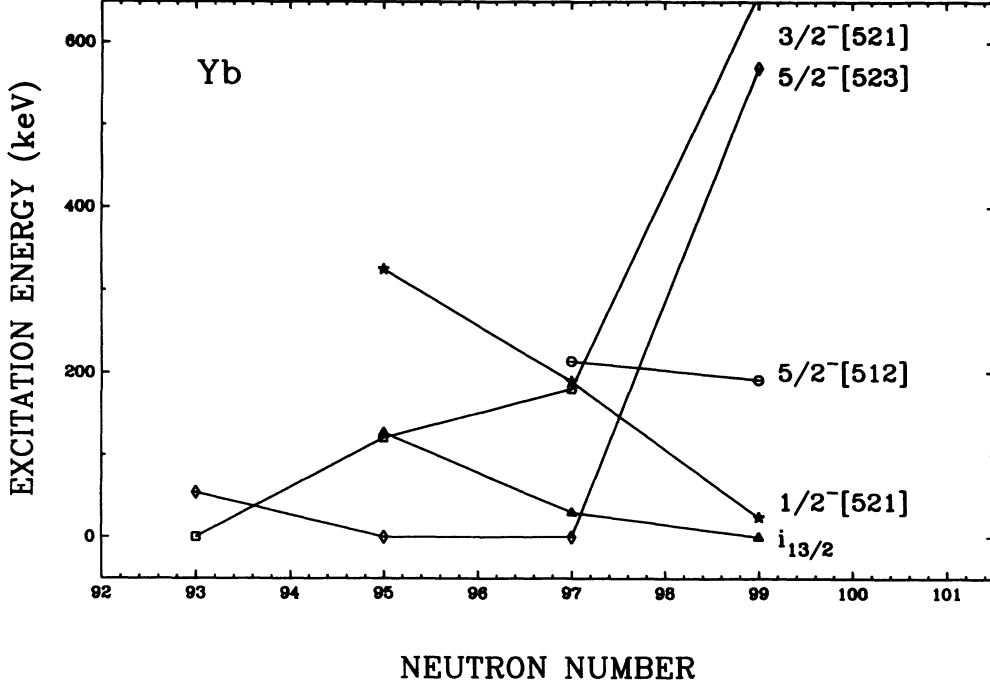


FIG. 7. Bandhead excitation energies for odd Yb isotopes.

ton and neutron single-qp energies are added to obtain the spectrum of  $^{166}\text{Lu}$  (the residual proton-neutron interaction which can split the  $K_{\geq} = |\Omega_p \pm \Omega_n|$  states, according to the Gallagher-Moszkowski coupling rules [25], is neglected). This zero-order set of energies most likely provides a complete level scheme for  $^{166}\text{Lu}$  up to  $\approx 500$  keV.

In order to attempt an identification of the proton and neutron orbitals associated with a given rotational band in a doubly odd nucleus, especially when the experimental information is incomplete, one needs a qualitative understanding of the different ways the valence nucleons couple together. Such a classification scheme has been proposed [7,11,26] and shall be used here.

We begin the discussion with the *B* band because it is the most intense and its interpretation seems to be clear, providing constraints for the spins of the lower-lying states.

#### A. *B* Band

The configuration proposed for this band is  $\tilde{\pi}_{\frac{1}{2}^-}[514] \otimes \tilde{\nu}i_{13/2}(\frac{5}{2}^+[642])$ . Band *B* exhibits a value of 0.7 for the  $K_1$  parameter. This parameter corresponds to an effective projection quantum number  $K$  and is obtained as follows: From the expression for the energies of the states belonging to a rotational band

$$E(I) = (\hbar^2/2\mathcal{J})[I(I+1) - K^2], \quad (1)$$

one calculates the ratio between the two first  $\Delta I = 1$  transitions to be

$$X = \frac{E(K+2) - E(K+1)}{E(K+1) - E(K)} = \frac{K+2}{K+1} \quad (2)$$

and a  $K$  value, denoted  $K_1$ , is extracted

$$K_1 = \frac{(2-X)}{(X-1)}. \quad (3)$$

The  $K_1$  value and the difference between this parameter and the expected projection quantum number  $K$  is a characteristic of each rotational structure.  $K_1 = 0.7$  is too small except for a highly compressed band [7]. Compression means that the first dipole transition is much smaller than the second one as compared to the situation in a high- $K$  normal band (still another possibility would be to admit a small  $K$  band, but this would be very difficult to accommodate in the level scheme.) Furthermore, the *B* band shows a definite level staggering. This behavior can arise in a doubly odd nucleus when a signature-split excitation combines with the favored signature component of a band which has an even larger signature splitting [11] (as, for example, in a decoupled band). In the present case this behavior can arise from either the  $\tilde{\nu}i_{13/2}$  or the  $\tilde{\pi}_{\frac{1}{2}^-}[514]$  orbitals which both have some signature splitting (actually the splitting of the *B* band is comparable to the one in the  $\tilde{\pi}_{\frac{1}{2}^-}[514]$  band while it is much larger for the  $\tilde{\nu}i_{13/2}$  structure). The first option, i.e., a structure associated with the two  $\tilde{\nu}i_{13/2}$  signatures, requires that the proton occupies a decoupled orbital ( $\tilde{\pi}_{\frac{1}{2}^+}[411]$  or  $\frac{1}{2}^-[541]$ ). This is not satisfactory because the  $\tilde{\nu}i_{13/2}$  bands in both  $^{165}\text{Yb}$  and  $^{167}\text{Hf}$  correspond to decoupled bands. We expect, for the  $\tilde{\pi}(\text{decoupled}) \otimes \tilde{\nu}i_{13/2}$  structure, an almost doubly decoupled band [11] (cf. *C* and *D* bands).

The second option involves the two  $\tilde{\pi}_{\frac{1}{2}^-}[514]$  signatures. This orbital exhibits staggering in the light Lu, Ta, and Re isotopes partially due to the high- $j$  ( $h_{11/2}$ ) value

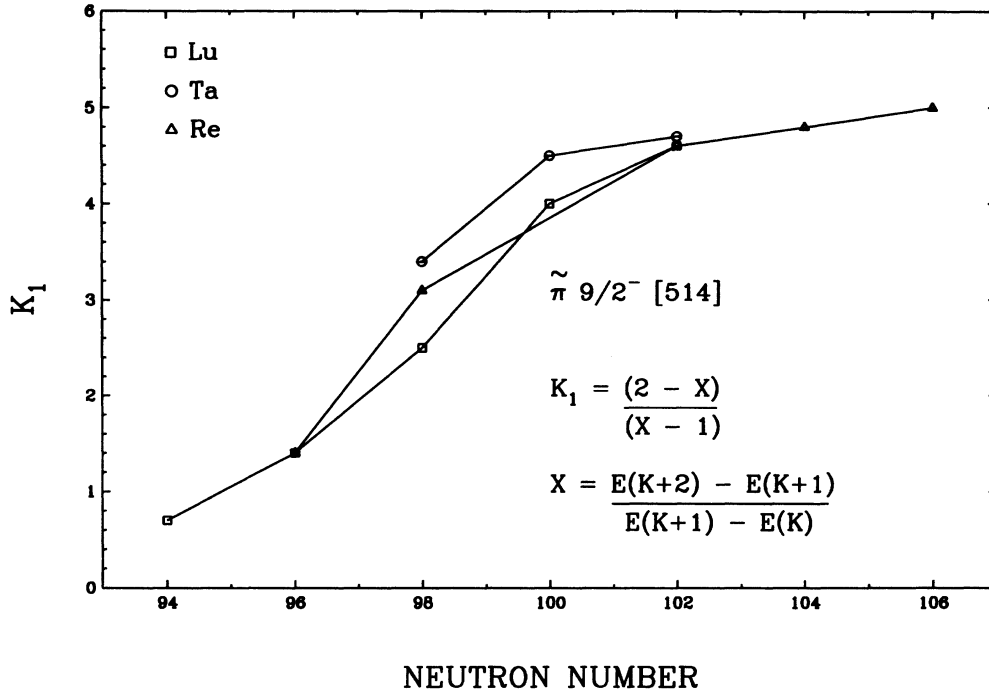


FIG. 8. Effective projection quantum number  $K_1$  vs neutron number for the  $\tilde{\pi} \frac{9}{2}^- [514]$  orbital.

and the possible presence of triaxiality in its structure.

Figure 8 displays the extracted  $K_1$  values for the  $\tilde{\pi} \frac{9}{2}^- [514]$  bands versus neutron number for the above-mentioned elements and it shows the anomalous behavior for the neutron-deficient isotopes (starting from a normal value of  $\approx 4.5$  for the heavy ones).

If the proton orbital associated with the  $B$  band is  $\frac{9}{2}^- [514]$  and its two signature components are present, the neutron orbital must correspond to a very distorted or decoupled band ( $\tilde{\nu} i_{13/2}(\frac{5}{2}^+ [642])$  or  $\tilde{\nu} \frac{1}{2}^- [521]$ ), and only its favored signature can participate. To decide between these two configurations the  $g$ - $S$  band-crossing frequencies can be studied. It is well known that these frequencies can be extracted from the intersection between the slopes of the Routhians in an  $(e', \omega)$  plot, before and after the alignment of two quasiparticles [13,27,28]. The Routhians  $e'$  have been calculated using a reference determined [9] for each band individually.

Table III lists the values obtained for some Yb (Refs. [15,22,23,29]), Lu (Ref. [16]), Hf (Refs. [29–33]), and Ta (Refs. [10,34]) isotopes. The differences between the experimental values corresponding to odd (and doubly odd) isotopes and their even-even cores,  $\delta \hbar \omega_{o,o-o} = \hbar \omega_{o,o-o} - \hbar \omega_{e-e}$ , are given as well as the calculated shifts for the odd-odd nuclei in terms of the corresponding odd-nucleus shifts,  $\delta \hbar \omega_{o-o}^c = \delta \hbar \omega_{o,p} + \delta \hbar \omega_{o,n}$ .

For even-even nuclei the crossing is observed around a rotational frequency  $\hbar \omega \approx 0.3$  MeV, and it is usually interpreted as the alignment of two  $i_{13/2}$  neutrons. In odd- $N$  nuclei the occupation of this orbital causes a delay in the crossing frequency due to blocking. If the occupied orbital is different from  $\tilde{\nu} i_{13/2}$  and since the pairing

correlations are smaller in the odd- $N$  system, less energy is needed to break a  $\tilde{\nu} i_{13/2}$  pair, giving rise to a smaller crossing frequency. The first backbending interpretation is, however, not unique [10,13] since the  $\tilde{\nu} i_{13/2}$  and  $\tilde{\pi} h_{9/2}(\frac{1}{2}^- [541])$  orbitals seem to play a similar role as far as shifts in crossing frequencies are concerned. In fact, we can see in Table III that there is an increase in the crossing frequency for the  $h_{9/2}$  bands of similar magnitude as for  $\tilde{\nu} i_{13/2}$  bands.

The crossing-frequency systematics [13] shows that the backbending in a  $\tilde{\pi} h_{9/2} \otimes \tilde{\nu} i_{13/2}$  semidecoupled band has the largest delay, presumably because the two critical orbitals are blocked. Still, an alternative explanation may be that the delay in crossing frequency in  $\tilde{\pi} h_{9/2}$  bands has to do with a larger deformation related to a polarization effect of the strongly prolate  $\frac{1}{2}^- [541]$  orbit [16]. This scenario is more likely to hold for the Lu case than for Re and Ir isotopes. In this context the delay of  $\hbar \omega$  in the  $\tilde{\pi} h_{9/2} \otimes \tilde{\nu} i_{13/2}$  band may be the result of the blocked lowest  $i_{13/2}$  crossing and a deformation-delayed second-lowest  $i_{13/2}$  crossing. Apparently the large interaction between the  $g$  and  $S$  bands in this structure manifests itself through a very smooth  $(e', \omega)$  curve and, generally, only a lower limit for  $\hbar \omega$  can be obtained. We can also observe a fair additivity in the crossing-frequency shifts  $\delta \hbar \omega_{o-o} \approx \delta \hbar \omega_p + \delta \hbar \omega_n$  in this structure, which is excellent in the case of doubly decoupled bands ( $\tilde{\pi} h_{9/2}(\frac{1}{2}^- [541]) \otimes \tilde{\nu} \frac{1}{2}^- [521]$ ). If we deblock one of the critical orbitals, the crossing frequency comes down, but remains greater than the one corresponding to the non-critical orbital. The compressed bands fall into this last category and we can distinguish between the

$\bar{\pi} \frac{9}{2}^- [514] \otimes \bar{\nu} (i_{13/2}$  or  $\frac{1}{2}^- [521])$  options, by examining whether the backbending in the  $B$  band is delayed or not with respect to the  $\bar{\pi} \frac{9}{2}^- [514]$  in  $^{165}\text{Lu}$ . In fact, the lower limit obtained for the crossing frequency indicates a strong delay attributable only to the  $i_{13/2}$  neutron. This delay is clearly observed in Fig. 9(b), where the experimental alignments for both signatures of band  $B$ , the core ( $^{164}\text{Yb}$ ) and  $\frac{9}{2}^- [514]$  bands ( $\alpha = \pm \frac{1}{2}$ ) belonging to  $^{165}\text{Lu}$  are plotted as a function of the rotational frequency. As will be shown in the next section, electromagnetic properties, however, do not show any significant differences for the two configurations. The state populated through the

85.5 keV transition must have even spin since the favored band in the  $\bar{\pi} \frac{9}{2}^- [514] \otimes \bar{\nu} i_{13/2} (\frac{5}{2}^+ [642])$  structure corresponds to even spins (signature=0). This lends additional support to the assertion on the existence of the 54 keV line suggested above.

### B. A Band

The configuration proposed for this band is  $\bar{\pi} \frac{7}{2}^+ [404] \otimes \bar{\nu} i_{13/2} (\frac{5}{2}^+ [642])$ . This structure has  $K_1 = 2.0$  and a moment of inertia which remains relatively constant at least for some initial portion of the band.

TABLE III. Crossing frequencies.

Nucleus	Band	$\alpha$	$\hbar\omega$ (MeV)	$\delta\hbar\omega$ (MeV)	$\delta\hbar\omega^c$ (MeV)
$^{164}\text{Yb}$	g.s.	0	0.285(10)		
$^{166}\text{Yb}$	g.s.	0	0.305(10)		
$^{166}\text{Hf}$	g.s.	0	0.295(10)		
$^{170}\text{Hf}$	g.s.	0	0.265(5)		
$^{172}\text{Hf}$	g.s.	0	0.290(10)		
$^{165}\text{Yb}$	$\frac{5}{2}^- [523]$	$+\frac{1}{2}$	0.235(5)	-0.050	
	$i_{13/2}$	$+\frac{1}{2}$	0.360(10)	+0.075	
		$-\frac{1}{2}$	> 0.310(10)	> +0.025	
$^{167}\text{Yb}$	$\frac{5}{2}^- [523]$	$+\frac{1}{2}$	0.245(5)	-0.060	
	$i_{13/2}$	$+\frac{1}{2}$	0.340(5)	+0.035	
$^{167}\text{Hf}$	$i_{13/2}$	$+\frac{1}{2}$	0.330(5)	+0.035	
$^{171}\text{Hf}$	$\frac{1}{2}^- [521]$	$+\frac{1}{2}$	0.220(5)	-0.045	
	$i_{13/2}$	$+\frac{1}{2}$	0.320(10)	+0.055	
$^{173}\text{Hf}$		$-\frac{1}{2}$	0.320(10)	+0.055	
	$\frac{1}{2}^- [521]$	$+\frac{1}{2}$	> 0.205(5)	> -0.085	
	$\frac{5}{2}^- [512]$	$+\frac{1}{2}$	> 0.180(5)	> -0.110	
$^{165}\text{Lu}$	$\frac{1}{2}^+ [411]$	$+\frac{1}{2}$	0.250(20)	-0.035	
		$-\frac{1}{2}$	0.240(5)	-0.045	
	$\frac{5}{2}^+ [402]$	$+\frac{1}{2}$	0.265(15)	-0.020	
	$\frac{7}{2}^+ [404]$	$\pm\frac{1}{2}$	0.275(5)	-0.010	
	$\frac{9}{2}^- [514]$	$\pm\frac{1}{2}$	0.280(10)	-0.005	
	$\frac{1}{2}^- [541]$	$+\frac{1}{2}$	0.330(5)	+0.045	
	$\frac{1}{2}^- [541]$	$+\frac{1}{2}$	0.310(10)	+0.045	
$^{171}\text{Ta}$	$\frac{5}{2}^+ [402]$	$+\frac{1}{2}$	0.250(5)	-0.015	
	$\frac{9}{2}^- [514]$	$\pm\frac{1}{2}$	0.260(10)	-0.005	
	$\frac{1}{2}^- [541]$	$+\frac{1}{2}$	0.340(10)	+0.050	
	$\frac{5}{2}^+ [402]$	$-\frac{1}{2}$	0.250(10)	-0.040	
$^{173}\text{Ta}$	$\frac{7}{2}^+ [404]$	$\pm\frac{1}{2}$	0.255(10)	-0.065	
	$\frac{9}{2}^- [514]$	$\pm\frac{1}{2}$	0.285(10)	-0.005	
	$A$	0,1	$\geq 0.290(5)$	$\geq +0.005$	+0.065
	$B$	0,1	$\geq 0.325(5)$	$\geq +0.040$	+0.070
$^{172}\text{Ta}^b$	$A$	0,1	$\geq 0.300(10)$	$\geq +0.035$	+0.050
	$B$	0,1	0.290(5)	+0.025	+0.040
	$C$	1	> 0.350(10)	> +0.085	+0.100
	$D$	0	> 0.285(10)	> +0.020	+0.100
	$D$	1	0.265(10)	0	0

<sup>a</sup>In  $^{166}\text{Lu}$  the  $A$  and  $B$  bands correspond to  $A \equiv \bar{\pi} \frac{7}{2}^+ [404] \otimes \bar{\nu} i_{13/2}$ ,  $B \equiv \bar{\pi} \frac{9}{2}^- [514] \otimes \bar{\nu} i_{13/2}$ .

<sup>b</sup>In  $^{172}\text{Ta}$  the  $A$ - $D$  bands correspond to  $A \equiv \bar{\pi} \frac{9}{2}^- [514] \otimes \bar{\nu} i_{13/2}$ ,  $B \equiv \bar{\pi} \frac{5}{2}^+ [402] \otimes \bar{\nu} i_{13/2}$ ,

$C \equiv \bar{\pi} h_{9/2} \otimes \bar{\nu} i_{13/2}$ ,  $D \equiv \bar{\pi} h_{9/2} \otimes \bar{\nu} \frac{1}{2}^- [521]$ .

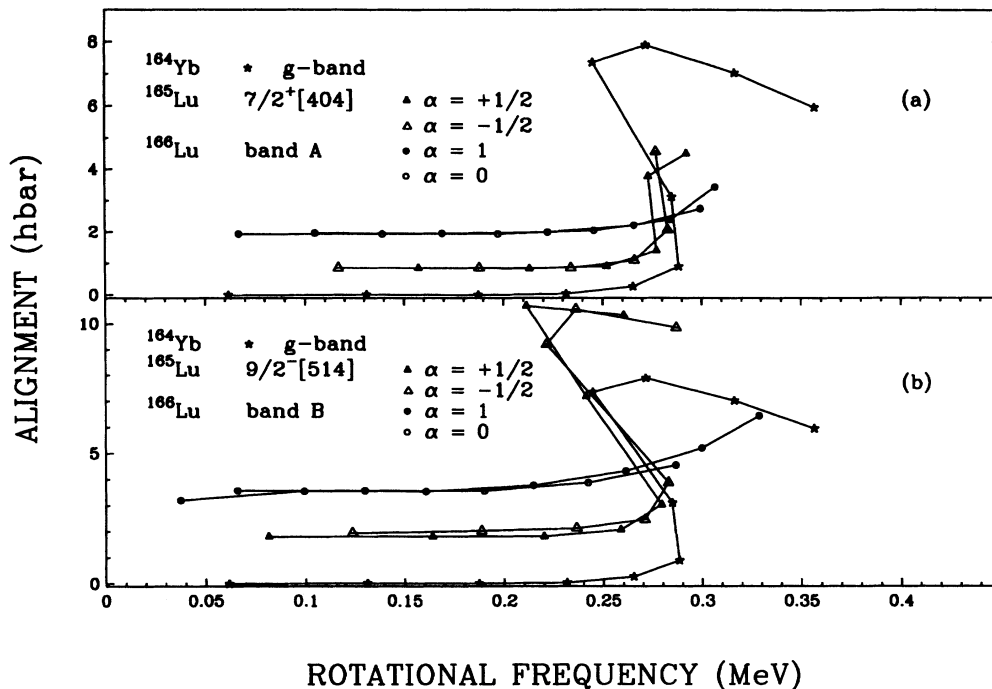


FIG. 9. Experimental alignments for (a)  $g$  band of  $^{164}\text{Yb}$ ,  $7/2^+[404]$  bands of  $^{165}\text{Lu}$ , and band  $A$  of  $^{166}\text{Lu}$ ; (b)  $g$  band of  $^{164}\text{Yb}$ ,  $9/2^-[514]$  bands of  $^{165}\text{Lu}$  and band  $B$  of  $^{166}\text{Lu}$ .

A low- $K$  normal coupling (namely, initial spin= $K=2$ ) is highly unlikely because fusion-evaporation reactions using heavy ions strongly favor the population of the near yrast region. In addition, the deexcitation of the  $B$  band restricts the spin of the state depopulated through the 61.3-keV transition to  $6^-, 7^-$  which would require the existence of nonobserved transitions connecting the  $A$  bandhead with this state, raising the bandhead energy and making it less competitive with other structures of higher spins. Hence, the most likely options are  $\bar{\pi} h_{9/2} \otimes \bar{\nu} (\frac{5}{2}^-[523], \frac{3}{2}^-[521], \frac{5}{2}^-[512])$ , and  $\bar{\pi} (\frac{5}{2}^+[402], \frac{7}{2}^+[404]) \otimes \bar{\nu} i_{13/2}$ , all these bands being of the compressed type. Only the third and fifth options have calculated  $B(M1)/B(E2)$  values (see next section) compatible with the experimental ones. Nevertheless, the last configuration is preferred because it renders unnecessary the assumption of unobserved transitions, the lower limit obtained for the crossing frequency [see Table III and Fig. 9(a)] falls into the systematics and it has higher spins placing itself nearer the yrast line.

### C. $C, D$ bands

The configuration proposed for these bands is  $\bar{\pi} h_{9/2} (\frac{1}{2}^-[541]) \otimes \bar{\nu} i_{13/2} (\frac{5}{2}^+[642])$ . These two bands, probably linked through the 162.4 and 251.3 keV transitions, represent one of the first observed cases [35] of semidecoupling in the limit of double decoupling [26]. This is due to the fact that the neutron Fermi level is located near the low- $\Omega$  orbitals in the  $\bar{\nu} i_{13/2}$  shell in this region, giving rise to decoupled bands in  $^{165}\text{Yb}$  and  $^{167}\text{Hf}$

and to a very distorted one in  $^{167}\text{Yb}$ .

The spins  $I^\pi = 7^-, 8^-$ , assigned to the observed low-lying states, is based on two arguments. The first one is the additivity of the alignments shown by the systematics for this kind of coupling. Thus, we obtain  $i_{o-o}^{\text{cal}} = i_p + i_n = 6.0$  from the alignments of the neighboring odd nuclei and  $i_{o-o}^{\text{exp}} = 5.9$  assigning  $I=7$  to the  $C$  bandhead. Another value for the initial spin would imply nonadditivity for the alignments. The second argument that supports these spin assignments is illustrated in Fig. 12 of Ref. [26] where a two-quasiparticle plus rotor model calculation has been performed for the  $\bar{\pi} h_{9/2} \otimes \bar{\nu} i_{13/2}$  structure. When the Fermi level is near the  $\Omega = \frac{5}{2}$  orbital, the low-spin states are very close in energy and in some cases inverted. This implies that the first transitions must have low energy, hence, be highly converted and very difficult to observe.

Odd (even) spins have been assigned to the  $C$  ( $D$ ) band because the  $C$  band is favored in energy (it is the strongest populated) and this favored band must be constructed from the favored proton and neutron signatures ( $\alpha_{o-o}^f = \alpha_p^f + \alpha_n^f = \frac{1}{2} + \frac{1}{2} = 1 \therefore$  odd spins), while the unfavored band ( $D$ ) corresponds to the coupling between the favored proton and the unfavored neutron signatures ( $\alpha_{o-o}^u = \alpha_p^f + \alpha_n^u = \frac{1}{2} - \frac{1}{2} = 0 \therefore$  even spins). We could not extract here a crossing frequency since the  $(e', \omega)$  curve does not exhibit a slope change, being compatible with the expected delay in the backbending for this kind of structure.

In addition, the  $(6^+)$  and  $(6^-)$  states, linked by the 61.3 keV transition, may be identified with the

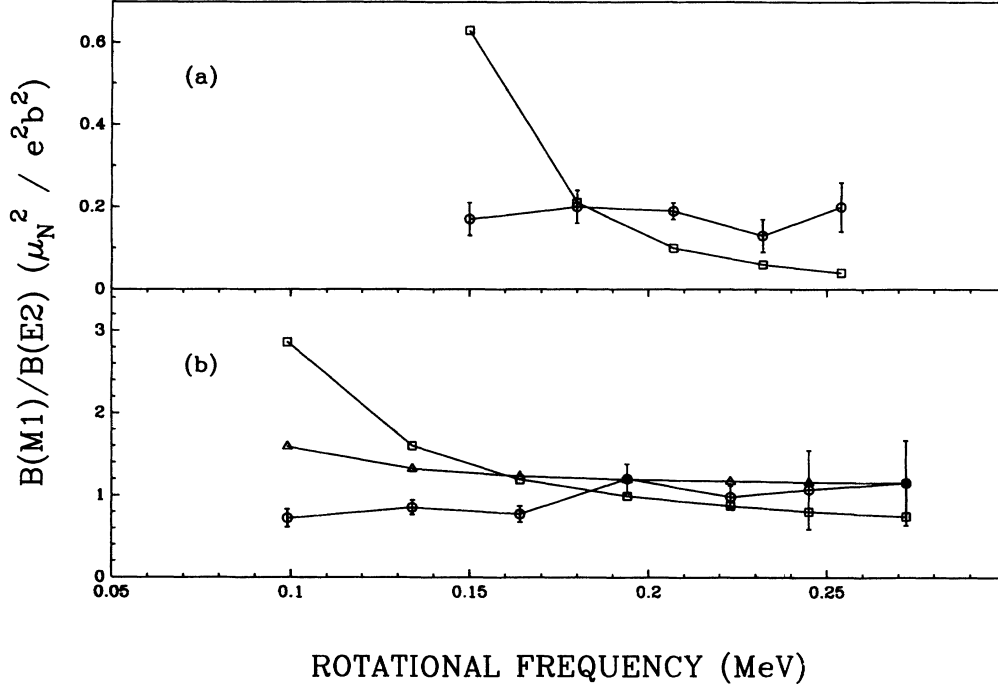


FIG. 10.  $B(M1)/B(E2)$  reduced transition probability ratios versus rotational frequency (a)  $\tilde{\pi}_{\frac{7}{2}^+}[404] \otimes \tilde{\nu} i_{13/2}$ ; (b)  $\tilde{\pi}_{\frac{9}{2}^-}[514] \otimes \tilde{\nu} i_{13/2}$ . Circles correspond to experimental values and squares to calculated ones in the framework of the cranking model. Triangles in (b) correspond to the calculated values for the  $\tilde{\pi}_{\frac{9}{2}^-}[514] \otimes \tilde{\nu}_{\frac{1}{2}^-}[521]$  configuration.

$\tilde{\pi}_{\frac{9}{2}^-}[514] \otimes \tilde{\nu}_{\frac{3}{2}^-}[521]$  and  $\tilde{\pi}_{\frac{7}{2}^+}[404] \otimes \tilde{\nu}_{\frac{5}{2}^-}[512]$  configurations, respectively.

## V. ELECTROMAGNETIC PROPERTIES

A useful method for studying electromagnetic properties in a rotational nucleus has been developed by Dönau and Frauendorf [36] in the framework of the cranking model. This method enables us to calculate  $B(M1)/B(E2)$  reduced transition probability ratios for a rotational band in a doubly odd nucleus from the experimental alignments of the bands corresponding to the involved proton and neutron orbitals of the neighboring odd nuclei.

We can express the transverse magnetic moment as

$$\begin{aligned} \mu_{\perp} = & (g_{Kp} - g_R)[\Omega_p(1 - K^2/I^2)^{1/2} - i_p K/I] \\ & + (g_{Kn} - g_R)[\Omega_n(1 - K^2/I^2)^{1/2} - i_n K/I], \end{aligned} \quad (4)$$

where the gyromagnetic factor associated with the collective rotational angular momentum  $R$  is  $g_R = 0.3$  and with the intrinsic single-particle angular momentum projection  $K$  for an almost pure- $\Omega$  excitation [37] is

$$g_K = g_{\Omega} = g_l + (g_s - g_l)\langle S_3 \rangle / \Omega. \quad (5)$$

For the orbital and spin  $g$  factors we use  $g_{l,p} = 1$ ;  $g_{s,p} \approx 3.91$ ;  $g_{l,n} = 0$ ; and  $g_{s,n} \approx -2.68$ , and  $\langle S_3 \rangle$  is the expectation value for the spin projection on the symmetry axis. The alignments  $i_p, i_n$  are calculated as described in Ref. [9].

The  $B(M1)$  and  $B(E2)$  are, in units of  $\mu_N^2$  and  $e^2 b^2$ , respectively,

$$B(M1, I \rightarrow I-1) = |\langle II | \mu(M1) | I-1 I-1 \rangle|^2 = (3\mu_1^2)/(8\pi), \quad (6)$$

$$\begin{aligned} B(E2, I \rightarrow I-2) &= \frac{5}{16\pi} Q_0^2 \langle IK20 | I-2K \rangle^2 \\ &= \frac{45(I+K)(I+K-1)(I-K)(I-K-1)Q_0^2}{4\pi(2I+1)(2I)(2I-1)(2I-2)}. \end{aligned} \quad (7)$$

The intrinsic quadrupole moment  $Q_0$  is calculated for a  $(Z, A)$  nucleus with quadrupole deformation  $\beta$  as

$$Q_0 = 1.44 \times 10^{-2} \left( \frac{9}{5\pi} \right)^{1/2} Z A^{2/3} \beta (1 + 0.16\beta) \text{ b}. \quad (8)$$

We can obtain an estimate for the deformation  $\beta$  from the neighboring  $(Z, A)$  even-even nuclei if information about the half-life ( $T$ ) of the first  $2^+$  state is available,

$$\beta = -3.125 + \left[ 9.766 + \frac{1.163 \times 10^{-3}}{Z A^{2/3} E^{5/2} T^{1/2} (1 + \alpha)^{1/2}} \right]^{1/2}, \quad (9)$$

where  $\alpha$  is the total conversion coefficient for the  $2^+ \rightarrow 0^+$  transition (its energy  $E$  and half-life are expressed in MeV and s, respectively).

The  $B(M1)/B(E2)$  values can be compared with the experimental ones obtained from

$$B(M1)/B(E2) = 0.693(1 + \delta^2)^{-1} R (E_{\gamma_2}^5 / E_{\gamma_1}^3). \quad (10)$$

$E_{\gamma_1, \gamma_2}$  are the transition energies corresponding to  $\Delta I = 1, 2$ , respectively.  $R$  is the  $I(\gamma_1)/I(\gamma_2)$   $\gamma$ -ray intensity ratio and the mixing ratio  $\delta$  is obtained, provided  $I \gg K$ , as

$$\delta = 0.9308 E_{\gamma} Q_0 K [I^2 - K^2]^{1/2} / (\mu_1 I^2). \quad (11)$$

In this framework we have calculated  $B(M1)/B(E2)$

ratios for the configurations included in the zero-order level scheme. The results for those corresponding to  $A$  and  $B$  bands are plotted in Figs. 10(a) and (b) and compared with the experimental values. Also, in Fig. 10(b) the calculated values for the  $\tilde{\pi} \frac{9}{2}^- [514] \otimes \tilde{\nu} \frac{1}{2}^- [521]$  configuration are shown.

## VI. CONCLUSIONS

A completely new high-spin level scheme for  $^{166}\text{Lu}$  is proposed. Each band has been identified on the basis of the coupling systematics for doubly odd nuclei belonging to the heavy rare-earth region. For this purpose effective projection quantum numbers  $K_1$ , alignments, and crossing frequencies have been extracted and  $B(M1)/B(E2)$  ratios have been calculated and compared with the experimental values. The importance of the  $\tilde{\nu} i_{13/2}$  orbital manifests itself through its presence in all the structures found.

A similar investigation has been carried at Oak Ridge National Laboratory [38].

## ACKNOWLEDGMENTS

Partial support from the Fundacion Antorchas is gratefully acknowledged. Three of us, E.W.C., P.P., and W.A.S., wish to thank the hospitality of the Tandem Laboratory and the support of the ICTP. A.J.K., M. Davidson, and J.D. are members of CONICET.

- 
- [1] A. J. Kreiner, M. Fenzl, S. Lunardi, and M. A. J. Mariscotti, Nucl. Phys. **A282**, 243 (1977).
- [2] A. J. Kreiner, C. Baktash, G. García Bermúdez, and M. A. J. Mariscotti, Phys. Rev. Lett. **47**, 1709 (1981), and references therein.
- [3] A. J. Kreiner, D. E. Digregorio, A. J. Fendrik, J. Davidson and M. Davidson, Phys. Rev. C **29**, 1572 (1984); Nucl. Phys. **A432**, 451 (1985).
- [4] A. J. Kreiner, J. Davidson, M. Davidson, P. Thieberger, E. K. Warburton, S. André, and J. Genevey, Nucl. Phys. **A489**, 525 (1988), and references therein.
- [5] A. J. Kreiner, J. Davidson, M. Davidson, P. Thieberger, and E. K. Warburton, Phys. Rev. C **42**, 878 (1990).
- [6] J. Davidson, M. Davidson, M. Debray, G. Falcone, D. Hojman, A. J. Kreiner, I. Mayans, C. Pomar, and D. Santos, Z. Phys. A **324**, 363 (1986).
- [7] A. J. Kreiner, J. Davidson, M. Davidson, D. Abriola, C. Pomar, and P. Thieberger, Phys. Rev. C **36**, 2309 (1987); **37**, 1338 (1988).
- [8] D. Santos, A. J. Kreiner, J. Davidson, M. Davidson, M. Debray, D. Hojman, and G. Falcone, Phys. Rev. C **39**, 902 (1989).
- [9] A. J. Kreiner and D. Hojman, Phys. Rev. C **36**, 2173 (1987).
- [10] A. J. Kreiner, D. Hojman, J. Davidson, M. Davidson, M. Debray, G. Falcone, D. Santos, C. W. Beausang, D. B. Fossan, R. Ma, E. S. Paul, S. Shi, and N. Xu, Phys. Lett. B **215**, 629 (1988).
- [11] A. J. Kreiner, in *Proceedings of the International Conference on Contemporary Topics in Nuclear Structure Physics, Cocoyoc, Mexico, 1988*, edited by R. F. Casten, A. Frank, M. Moshinsky, and S. Pittel (World Scientific, Singapore, 1988), p. 521, and references therein.
- [12] F. S. Stephens and R. S. Simon, Nucl. Phys. **A183**, 257 (1972).
- [13] A. J. Kreiner, Nucl. Phys. **A520**, 225c (1990).
- [14] D. Hojman, A. J. Kreiner, M. Davidson, J. Davidson, M. Debray, E. Cybulska, P. Pascholati, and W. Seale, in *Proceedings of the XII Workshop on Nuclear Physics, Cataratas del Iguazú, Argentina, 1989*, edited by M. C. Cambiaggio, A. J. Kreiner, and E. Ventura (World Scientific, Singapore, 1989), p. 360.
- [15] F. W. N. De Boer, P. F. A. Goudsmit, P. Koldewijn, and B. J. Meyer, Nucl. Phys. **A225**, 317 (1974).
- [16] S. Jónsson, J. Lyttkens, L. Carlén, N. Roy, H. Ryde, W. Walús, J. Kownacki, G. B. Hagemann, B. Herskind, J. D. Garrett, and P. O. Tjom, Nucl. Phys. **A422**, 397 (1984).
- [17] D. Barnéoud and C. Foin, Nucl. Phys. **A287**, 77 (1977).
- [18] K. E. G. Löbner, in *The Electromagnetic Interaction in Nuclear Spectroscopy*, edited by W. D. Hamilton (North-Holland, Amsterdam, 1975), p. 215 and 164.
- [19] C. Foin, D. Barnéoud, S. A. Hjorth and R. Bethoux, Nucl. Phys. **A199**, 129 (1973).
- [20] P. Kemnitz, L. Funke, K. H. Kaun, H. Sodan, G. Winter, and M. I. Baznat, Nucl. Phys. **A209**, 271 (1973).
- [21] J. Kownacki, J. D. Garrett, J. J. Garrdhoje, G. B.

- Hagemann, B. Herskind, S. Jónsson, N. Roy, H. Ryde, and W. Walús, *Nucl. Phys.* **A394**, 269 (1983).
- [22] E. M. Beck, J. C. Bacelar, M. A. Delaplanque, R. M. Diamond, F. S. Stephens, J. E. Draper, B. Herskind, A. Holm, and P. O. Tjom, *Nucl. Phys.* **A464**, 472 (1987).
- [23] N. Roy, S. Jónsson, H. Ryde, W. Walús, J. J. Gaardhoje, J. D. Garrett, G. B. Hagemann, and B. Herskind, *Nucl. Phys.* **A382**, 125 (1982).
- [24] V. S. Shirley, *Nucl. Data Sheets* **36**, 467 (1982).
- [25] C. J. Gallagher, Jr. and S. A. Moszkowski, *Phys. Rev.* **111**, 1282 (1958).
- [26] A. J. Kreiner, in *Proceedings of the XII Workshop on Nuclear Physics, Cataratas del Iguazú, Argentina, 1989*, edited by M. C. Cambiaggio, A. J. Kreiner and E. Ventura (World Scientific, Singapore, 1989), p. 137.
- [27] J. D. Garrett, in *Proceedings of the Conference on High Angular Momentum Properties of Nuclei, Oak Ridge, USA, 1982*, edited by N. Johnson (Harwood Academic, Chur, Switzerland, 1982), p. 17.
- [28] A. J. Kreiner, V. R. Vanin, F. A. Beck, Ch. Bourgeois, Th. Byrski, D. Curien, G. Duchene, B. Haas, J. C. Merdinger, M. G. Porquet, P. Romain, S. Rouabah, D. Santos, and J. P. Vivien, *Phys. Rev. C* **40**, 487 (1989).
- [29] *Table of Isotopes*, edited by C. M. Lederer and V. S. Shirley (Wiley, New York, 1978).
- [30] V. S. Shirley, *Nucl. Data Sheets* **58**, 900 (1989).
- [31] V. S. Shirley, *Nucl. Data Sheets* **43**, 162 (1984).
- [32] V. S. Shirley, *Nucl. Data Sheets* **54**, 609 (1988).
- [33] A. E. Ignatovich, E. N. Shurshikov, and Yu. F. Jaborov, *Nucl. Data Sheets* **52**, 383 (1987).
- [34] J. C. Bacelar, R. Chapman, J. R. Leslie, J. C. Lisle, J. N. Mo, E. Paul, A. Simcock, J. C. Willmott, J. D. Garrett, G. B. Hagemann, B. Herskind, A. Holm, and P. M. Walker, *Nucl. Phys.* **A442**, 547 (1985).
- [35] S. André, D. Bernéoud, C. Foin, J. Genevey, J. A. Pinston, B. Haas, J. P. Vivien, and A. J. Kreiner, *Z. Phys. A* **333**, 247 (1989).
- [36] F. Döna and S. Frauendorf, in *Proceedings of the Conference on High Angular Momentum Properties of Nuclei, Oak Ridge, Tennessee, 1982*, edited by N. Johnson (Harwood Academic, Chur, Switzerland, 1982), p. 143.
- [37] A. Bohr and B. Mottelson, in *Nuclear Structure* (Benjamin, Reading, Mass., 1975), Vol. 2, p. 302.
- [38] J. McNeill, C. Baktash, and J. D. Garrett, private communication.